State-Dependent Cocaine Block of Sodium Channel Isoforms, Chimeras, and Channels Coexpressed with the β1 Subunit

Sterling N. Wright,* Sho-Ya Wang,# Yong-Fu Xiao,§ and Ging Kuo Wang*

*Department of Anesthesia Research Laboratories, Harvard Medical School, Brigham and Women's Hospital, Boston, Massachusetts 02115; #Department of Biology, State University of New York at Albany, Albany, New York 12222; and §Department of Medicine, Harvard Medical School, Beth Israel Deaconess Medical Center, Boston, Massachusetts 02215 USA

ABSTRACT Cocaine block of human cardiac (hH1) and rat skeletal (μ1) muscle sodium channels was examined under whole-cell voltage clamp in transiently transfected HEK293t cells. Low affinity block of resting μ1 and hH1 channels at −180 mV was the same, and high affinity block of inactivated channels at −70 mV was the same. Cocaine block of hH1 channels was greater than block of μ1 channels at voltages between −120 mV and −90 mV, suggesting that greater steady-state inactivation of hH1 channels in this voltage range makes them more susceptible to cocaine block. We induced shifts in the voltage dependence of steady-state inactivation at μ1 and hH1 channels by constructing μ1/hH1 channel chimeras or by coexpressing the wild-type channels with the rat brain β1 subunit. In contrast to several previous reports, coexpression of the rat brain β1 subunit with μ1 or hH1 produced large positive shifts in steady-state inactivation. Shifts in the voltage dependence of steady-state inactivation elicited linear shifts in steady-state cocaine block, yet these manipulations did not affect the cocaine affinity of resting or inactivated channels. These data, as well as simulations used to predict block, indicate that state-dependent cocaine block depends on both steady-state inactivation and channel activation, although inactivation appears to have the predominant role.

INTRODUCTION

Sodium channels are voltage-sensitive membrane proteins that produce the action potentials in excitable tissues such as nerve, skeletal muscle, and cardiac muscle. With sufficient depolarization from the resting potential, sodium channels activate, open, and allow sodium ion flux. Within a few milliseconds of opening, the channels inactivate and return to a nonconducting state (Hodgkin and Huxley, 1952). The general structure of the sodium channel isoforms from different excitable tissues appears to be conserved (Catterall, 1995; Fozzard and Hanck, 1996). Sodium channel α subunits consist of four homologous domains (D1–D4), and each domain contains six transmembrane segments (S1–S6). The arrangement of the four domain regions in the membrane forms a pore for conducting sodium ions.

Although the structures of the different tissue isoforms of sodium channel are generally similar, there are marked differences among the isoforms in kinetic behavior and pharmacology. Compared to skeletal muscle sodium channels, cardiac sodium channels activate and inactivate at more negative membrane potentials and have a slower time constant of macroscopic current decay when expressed in mammalian cells (Wang et al., 1996a; Wright et al., 1997). Pharmacological differences between cardiac and skeletal muscle sodium channels include a relatively greater sensitivity of the cardiac muscle isoform to Cd^{2+} ions and a lower sensitivity to tetrodotoxin (Frelin et al., 1986). While the residues responsible for Cd^{2+} and tetrodotoxin block have been delineated (Tomaselli et al., 1995), sodium channel block by local anesthetics is less clearly understood because channel affinity profoundly varies depending on channel state.

The two principal models used to explain the state-dependent modulation of receptor affinity are the Modulated Receptor hypothesis (Hille, 1977) and the Guarded Receptor hypothesis (Starmer et al., 1984). In Hille's (1977) modulated receptor scheme, the inactivation particle (h gate) accounted for the state-dependent alterations in receptor affinity. In contrast, Starmer et al. (1984) attributed state-dependent alterations in receptor affinity to the activation particle (m gate). A clear determination of which mechanism is responsible for receptor modulation might help explain why some local anesthetics, such as cocaine or lidocaine, strongly affect cardiac physiology at concentrations that have little obvious effect on skeletal muscle physiology.

The purpose of the present study was to examine the mechanisms that influence channel affinity and state-dependent cocaine block of skeletal muscle and cardiac sodium channels. Two previous studies suggested that the anesthetic receptor in cardiac sodium channels has a higher affinity for lidocaine than does the receptor in skeletal muscle sodium channels, and that this difference in receptor affinity accounts for the difference in lidocaine sensitivity between cardiac and skeletal muscle tissue (Nuss et al., 1995b; Wang et al., 1996b). In contrast, we have recently shown that mammalian cardiac (hH1) and skeletal muscle sodium channels (μ1) have very similar affinities for co-

Received for publication 31 March 1998 and in final form 16 September 1998.

Address reprint requests to Dr. Sterling N. Wright, Department of Biological Sciences, Murray State University, P.O. Box 9, Murray, KY 42071. Tel.: 502-762-2087; Fax: 502-762-2788; E-mail: sterling.wright@murraystate.edu.

0006-3495/99/01/233/13 $2.00

caine and for lidocaine (Wright et al., 1997). At intermediate voltages (−120 mV to −90 mV), however, cocaine blocked hH1 channels with much greater potency, suggesting that the modulation of receptor affinity differs at the two isoforms. Although we lacked direct evidence to support our hypothesis, we suggested that cocaine blocked a larger proportion of hH1 channels than μ1 channels at intermediate voltages because of greater steady-state inactivation of the hH1 isoform (Wright et al., 1997). To test this hypothesis, we induced shifts in steady-state inactivation by creating μ1/hH1 channel chimeras and also by coexpressing the rat brain β1 subunit with the α subunits of hH1 or μ1. In stark contrast to data from other expression systems (Isom et al., 1992, 1995; Nuss et al., 1995a), we found that β1 subunit coexpression induced strong positive shifts in the steady-state inactivation of both hH1 and μ1 channels. When we plotted the midpoint voltages of steady-state cocaine block as a function of the midpoint voltages of either steady-state activation or inactivation, we found that the relationship between block and steady-state inactivation was linear, and that block was better correlated with steady-state inactivation than with activation. In simulations of block, steady-state cocaine block of each channel could be fairly well predicted by using the steady-state inactivation curve of each channel and the K_d values of resting and inactivated channels. The fit by the model was further improved by imposing an equilibrium shift in the steady-state inactivation curve. These data and the model suggested that the modulation of local anesthetic receptor affinity depends heavily on steady-state inactivation and perhaps to some extent on channel activation resulting from the coupling between inactivation and activation. Some of the presented data have appeared in an abstract (Wright et al., 1998).

MATERIALS AND METHODS

Solutions and chemicals

The extracellular solution used to perfuse HEK cells contained (in mM): 65 NaCl, 85 choline chloride, 2 $CaCl_2$, and 10 HEPES (titrated with tetramethyl ammonium hydroxide to pH 7.4). The pipette solution contained (in mM) 100 NaF, 30 NaCl, 10 EGTA, and 10 HEPES (titrated with cesium hydroxide to pH 7.2). Cocaine hydrochloride was purchased from Mallinckrodt, Inc. (St. Louis, MO), and was stored at −20°C as a 200 mM solution in distilled water. Final anesthetic concentrations were obtained by serial dilution from a 10 mM stock solution prepared in external bathing solution.

Construction of μ1/hH1 channel chimeras

For $\mu1_{(1-3)}hH1_{(4)}$, site-directed mutagenesis (Wang and Wang, 1997) was used to create a *Cla*I site at positions 3862–3867 of the μ1-cDNA1/AMP vector (the translation initiation site was at +1n) by converting C into T at position 3867n. The μ1-*Cla*I-3862 was further modified into μ1-*Cla*I-*Cla*I by introducing another *Cla*I site in the 3′ polylinker. This was achieved by the digestion of μ1-*Cla*I-3862 with *Sal*I, followed by a blunting reaction and ligation to the *Cla*I linker. hH1-*Cla*I was created by mutating the ATTGAC (4416–4421n) in the hH1 clone (Gellens et al., 1992) into a *Cla*I site: ATCGAT. The translation initiation site in the hH1 clone is at position +1n. The $\mu1_{(1-3)}hH1_{(4)}$ channel was cloned by ligating the large μ1 *Cla*I fragment (domains 1–3) to the small hH1 *Cla*I fragment (domain 3 and 4 cytoplasmic linker and domain 4).

The chimera, $\mu1_{(1)}hH1_{(2-4)}$, was created by using the *BsiW*I site (at positions 1328–1333) of μ1-cDNA1/AMP. This restriction site in μ1 is located at the 3′ end junction of the domain 1 S6 segment. Because hH1 lacks this *BsiW*I site, we performed site-directed mutagenesis at the 3′ end junction of the domain 1 S6 segment of hH1 (at positions 1252–1257) to create the clone hH1-*BsiW*I (hH1 also has a *BsiW*I restriction site in the 3′ polylinker). Three-way ligation was used to join DNA fragments: 1.7 Kb-*Hind*III-*BsiW*I from μ1-cDNA1/AMP, 4 Kb-*BsiW*I from hH1-*BsiW*I, and 5 Kb-*Hind*III-*BsiW*I from hH1-*BsiW*I. The orientations of $\mu1_{(1-3)}hH1_{(4)}$, $\mu1_{(1)}hH1_{(2-4)}$, and of two other channel chimeras ($hH1_{(1-3)}\mu1_{(4)}$ and $hH1_{(1)}\mu1_{(2-4)}$) were determined by restriction mapping and sequencing. Introduction of the restriction sites for chimera formation did not produce point mutations in either the μ1 or the hH1 portion of channel chimeras.

Channel expression in HEK 293t cells

The methods used for maintaining transformed human embryonic kidney (HEK 293t) cells and for transiently expressing μ1 (Trimmer et al., 1989) and hH1 (Gellens et al., 1992) were described in a previous paper (Wright et al., 1997). For transient expression of the α subunits of cloned channels in HEK cells, we prepared the following DNA solution (Cannon and Strittmatter, 1993): 1 μg CD8 (cell surface antigen) and 2–10 μg sodium channel cDNA clone in the pcDNA1/amp vector (Invitrogen, San Diego, CA) were prepared in 250 mM $CaCl_2$ and added to a test tube containing 0.36 ml Hanks' balanced salt (2×) solution (in mM: 274 NaCl, 40 HEPES, 12 dextrose, 10 KCl, 1.4 Na_2HPO_4, pH 7.05). After a 20-min incubation at 22°C, the DNA solution was added to a cell culture (in a TI-25 flask) that was 30–50% confluent. After 15 h at 37°C, the transfected cells were replated onto 35-mm culture dishes (which also served as recording chambers) containing 2 ml fresh DMEM supplemented with taurine (1%), penicillin/streptomycin (1%), and heat-inactivated fetal bovine serum (10%). For coexpression of the rat brain β1 subunit (Isom et al., 1992) with μ1 or hH1 α subunits, saturating levels (>10-fold molar excess) of β1 cDNA were used to ensure that the resulting macroscopic currents were produced by channels consisting of both α and β1 subunits.

Electrophysiology procedures and data analysis

Whole-cell voltage clamp (Hamill et al., 1981) of HEK cells was used to study macroscopic sodium currents at room temperature (23 ± 2°C). Electrode resistances ranged from 0.4 to 1.0 MΩ. Command voltages were programmed by pCLAMP software and delivered by a List EPC7 voltage clamp. Data were sampled at 50 kHz and were filtered at 5 kHz. After gigaohm seal formation and establishment of whole-cell voltage clamp, the cells were always dialyzed for 25–30 min before acquiring data. Time-dependent shifts in the midpoint voltage of sodium channel availability during our experiments (~30–60 min after membrane rupture) would have been ~5–7 mV (Wang et al., 1996a). The holding potential for all experiments was −140 mV. Most of the capacitative current was canceled by the EPC7 circuitry. The remaining capacitative artifact and the leakage current were subtracted by the P/−4 method. The P/−4 method was not used for studies of use-dependent cocaine block. Voltage errors at +30 mV were ≤5 mV after 30–50% compensation. Least-squares curve fitting was performed with Microcal Origin software. Depending on the experiment, data were fitted by an empirical Boltzmann function $\{1/[1 + \exp((V_{0.5} - V)/k)]\}$, where $V_{0.5}$ is the midpoint voltage of the function and k is the slope factor (in mV/e-fold change in current); by a single exponential function $\{y_0 + A1*[1-\exp(-x/\tau1)]\}$; or by the sum of two exponential functions $\{y_0 + A1*[1-\exp(-x/\tau1)] + A2*[1-\exp(-x/\tau2)]\}$. Data are presented as mean ± SE.

RESULTS

Role of domain regions in sodium channel activation and inactivation

Previous studies indicated that steady-state inactivation of μ1/hH1 channel chimeras differed from the steady-state inactivation of the wild-type isoforms (Makita et al., 1996; Chahine et al., 1996; Benzinger et al., 1997). Our goal was to induce voltage-dependent shifts in steady-state channel activation or inactivation in an attempt to determine how shifts in channel kinetics might affect steady-state cocaine block. Fig. 1 *A* shows current records obtained from the two wild-type sodium channels, μ1 and hH1, and from two channel chimeras. The μ1 panel shows the four domains (D1–D4) of the sodium channel α subunit, the charged (+) S4 segments in each domain, and the amino and carboxyl termini. The channel chimera, $\mu1_{(1-3)}hH1_{(4)}$, contained domains 1–3 from the μ1 α subunit and domain 4 from the hH1 α subunit, whereas $\mu1_{(1)}hH1_{(2-4)}$ contained domain 1 from μ1 and domains 2–4 from hH1. Despite repeated attempts, two other channel chimeras, $hH1_{(1)}\mu1_{(2-4)}$ and $hH1_{(1-3)}\mu1_{(4)}$, failed to express current. To evoke the currents shown in Fig. 1 *A*, we delivered 10-ms step depolarizations from a holding potential of −140 mV. The inward currents for μ1, $\mu1_{(1-3)}hH1_{(4)}$, and $\mu1_{(1)}hH1_{(2-4)}$ channels peaked at −30 mV, whereas the peak inward current for hH1 channels occurred at −40 mV. The time dependence of macroscopic current decay for both $\mu1_{(1-3)}hH1_{(4)}$ and $\mu1_{(1)}hH1_{(2-4)}$ channels clearly resembled the decay of hH1 currents, which decayed more slowly than the μ1 current. At +30 mV, μ1 current decayed with a time constant of 0.28 ± 0.01 ms (n = 7). In contrast, hH1, $\mu1_{(1-3)}hH1_{(4)}$, and $\mu1_{(1)}hH1_{(2-4)}$ currents decayed with time constants of 0.49 ± 0.03 ms (n = 6), 0.46 ± 0.02 ms (n = 11), and 0.41 ± 0.01 ms (n = 13), respectively.

Parts *B* and *C* in Fig. 1 show the normalized membrane conductance and steady-state inactivation curves, respectively, for $\mu1_{(1-3)}hH1_{(4)}$ and $\mu1_{(1)}hH1_{(2-4)}$ channels. These data were fitted with an empirical Boltzmann function (*solid lines*) to determine the midpoint voltage ($V_{0.5}$) and the slope factor (k). For comparison, the fitted Boltzmann functions (*dotted lines*) for hH1 and μ1 channels (Wright et al., 1997) are also shown in parts *B* and *C*. The activation (i.e., the conductance-voltage relationship) of both $\mu1_{(1-3)}hH1_{(4)}$ and $\mu1_{(1)}hH1_{(2-4)}$ channels more closely resembled the activation of μ1 channels (Fig. 1 *B*). The $V_{0.5}$ value of channel activation for hH1 channels was significantly ($p < 0.05$; t-test) more negative than were the $V_{0.5}$ values of activation for μ1, $\mu1_{(1-3)}hH1_{(4)}$, or $\mu1_{(1)}hH1_{(2-4)}$ channels, whereas the $V_{0.5}$ values of activation for $\mu1_{(1-3)}hH1_{(4)}$ or $\mu1_{(1)}hH1_{(2-4)}$ were not significantly different ($p > 0.05$) from that of μ1 (Table 1).

We examined the steady-state inactivation properties of these four sodium channel isoforms by using a standard h_∞ pulse protocol. We delivered 100 ms conditioning pulses of various amplitudes and measured the available sodium current during a test pulse to +30 mV (Fig. 1 *C, inset*). The plot in Fig. 1 *C* shows the averaged data for the channel chimeras and the solid lines represent the fits by a Boltzmann function. The dotted lines are the fits to the averaged hH1 and μ1 data. The $V_{0.5}$ values of steady-state inactivation of $\mu1_{(1-3)}hH1_{(4)}$ and $\mu1_{(1)}hH1_{(2-4)}$ channels fell between the $V_{0.5}$ values of inactivation for hH1 and μ1, with $\mu1_{(1-3)}hH1_{(4)}$ more closely resembling μ1 and $\mu1_{(1)}hH1_{(2-4)}$ more closely resembling hH1 (Table 1). Consistent with a previous report that used the oocyte expression system to examine inactivation (Makita et al., 1996), the data in Fig. 1 *C* suggest that all four domain regions contribute, perhaps equally, to the voltage dependence of steady-state inactivation.

Cocaine block of μ1, hH1, and chimeras

As described above, chimera formation had distinct effects on channel activation and steady-state inactivation. The $V_{0.5}$ values of activation for both channel chimeras resembled that of μ1, but the $V_{0.5}$ values of steady-state inactivation for the chimeras were intermediate to those of μ1 and hH1. We compared the steady-state cocaine block of the four channels to perhaps distinguish whether the inactivation phenotype or the activation phenotype has the more prominent role in determining steady-state cocaine block. Cocaine binds to the channels with a stoichiometry of 1:1, so we measured 30 μM cocaine block of the channels over a 110 mV range of conditioning voltages. By using this approach, we were able to examine block of resting channels at the most negative conditioning voltages, block of inactivated channels at the least negative voltages, and block of varying proportions of resting and inactivated channels at intermediate voltages. The pulse protocol (Fig. 1 *D, inset*) consisted of a 10-s conditioning pulse ranging from −180 mV to −70 mV followed by a 100-ms interval at the holding potential and a subsequent test pulse to +30 mV. As previously described (Wright et al., 1997), a conditioning pulse of 10 s was necessary and sufficient for cocaine block to reach steady state at all of the channels in the study (n = 2–3 cells; data not shown). A 100-ms interval inserted between the conditioning pulse and the test pulse allowed drug-free channels to recover from fast inactivation. To normalize the data at each conditioning voltage, we divided the peak current amplitude at the test pulse in the presence of cocaine by the peak current amplitude elicited by the test pulse in control saline. At strongly negative conditioning pulses, 30 μM cocaine blocked ~10% of the resting $\mu1_{(1-3)}hH1_{(4)}$ and $\mu1_{(1)}hH1_{(2-4)}$ channels, which was similar to the block of resting μ1 and hH1 channels. When the channel chimeras were inactivated by a 10-s conditioning pulse to −70 mV, 30 μM cocaine blocked ~75–80% of the channels, which was similar to the block of inactivated μ1 and hH1 channels. As with the wild-type channels, 300 μM cocaine blocked ~55% of the resting channels and ~97% of the inactivated channels (Wright et al., 1997). At −180 mV, 300 μM cocaine blocked 55.5 ± 1.7% (n = 5) of

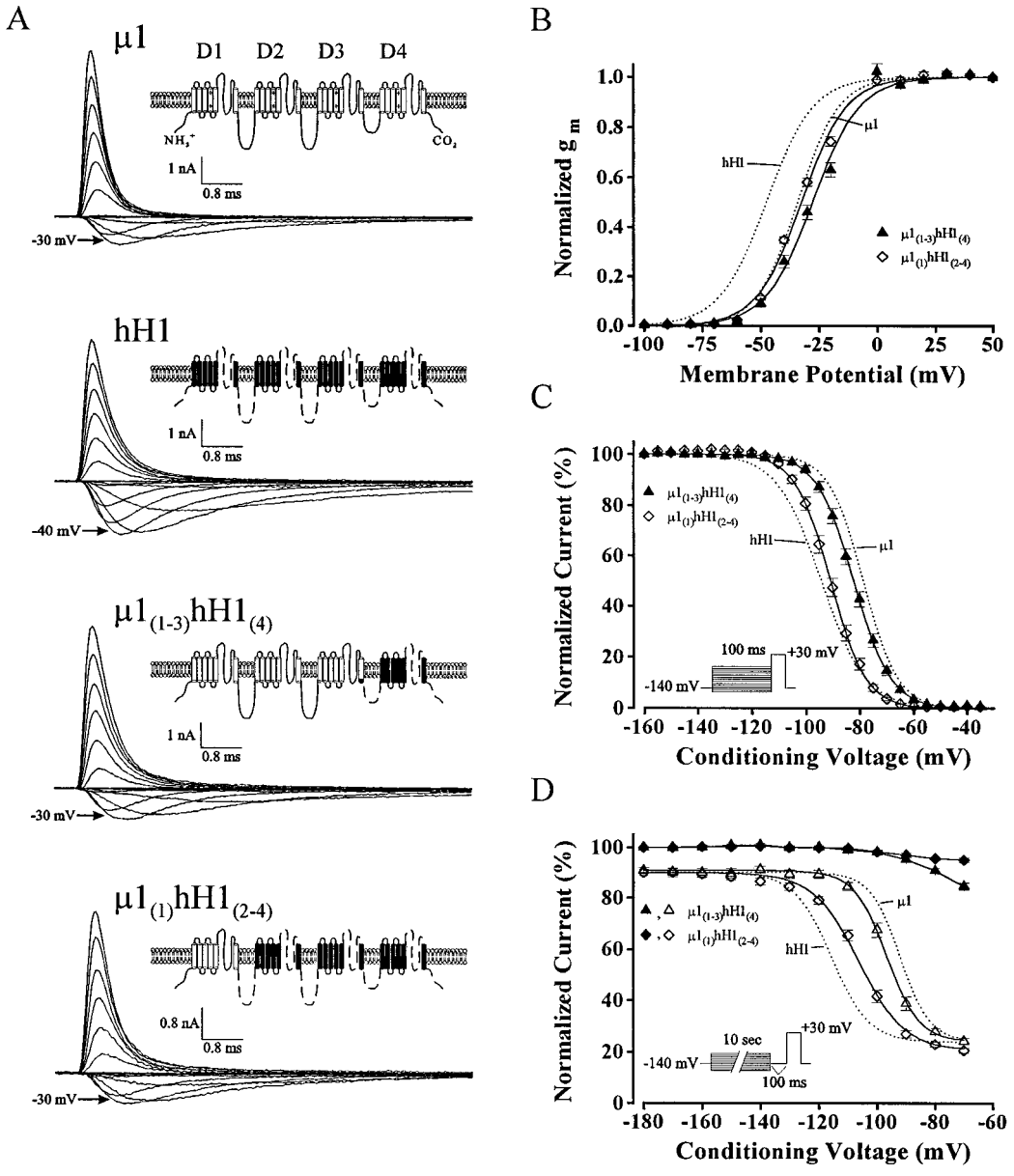

FIGURE 1 Activation, steady-state inactivation, and cocaine block of μ1, hH1, and μ1/hH1 channel chimeras. (*A*) The sodium channel α subunit structures and associated currents recorded from the two wild-type sodium channel isoforms, μ1 and hH1, and from two μ1/hH1 channel chimeras, $\mu1_{(1-3)}hH1_{(4)}$ and $\mu1_{(1)}hH1_{(2-4)}$, are shown. In the μ1 panel, the domain regions, the charged (+) voltage sensing regions, and the amino and carboxyl termini are labeled. The channel chimera, $\mu1_{(1-3)}hH1_{(4)}$, consisted of domains 1–3 from μ1 and the interdomain linker between domains 3 and 4 and domain 4 from hH1, whereas $\mu1_{(1)}hH1_{(2-4)}$ consisted of domain 1 from μ1 and domains 2–4 from hH1. The currents were evoked by 10-ms pulses from −140 mV to voltages ranging from −100 mV to +50 mV. The peak inward current and its corresponding voltage are labeled. (*B*) Normalized membrane conductance (g_m) plotted versus the amplitude of the 10-ms voltage step; g_m was determined from the equation $g_m = I_{Na}/(E_m - E_{Na})$, and the plot was fitted with a standard Boltzmann function. For clarity, only the fits to the μ1 and hH1 data are shown. For μ1, the average midpoint voltage ($V_{0.5}$) and slope (k) of the function were −32.8 ± 2.8 mV and 9.3 ± 1.5 mV, respectively. $V_{0.5}$ and k were: −48.0 ± 1.8 mV and 9.4 ± 0.9 mV, respectively, for hH1; −27.8 ± 1.2 mV and 9.8 ± 0.3 mV, respectively, for $\mu1_{(1-3)}hH1_{(4)}$; and −32.4 ± 0.6 mV and 9.7 ± 0.6 mV, respectively, for $\mu1_{(1)}hH1_{(2-4)}$. (*C*) Normalized sodium current availability function (h_∞) for the four channels. The pulse protocol is shown in the inset. The dotted lines are the fits to the averaged μ1 or hH1 data, as labeled. The average $V_{0.5}$ values (50% availability) and k values for the fitted Boltzmann functions were: −78.5 ± 1.0 mV and 6.1 ± 0.3 mV, respectively for μ1; −94.1 ± 1.4 mV and 7.7 ± 0.1 mV, respectively, for hH1; −82.2 ± 1.0 mV and 6.5 ± 0.2 mV, respectively, for $\mu1_{(1-3)}hH1_{(4)}$; and −90.7 ± 1.0 mV and 6.1 ± 0.1 mV, respectively, for $\mu1_{(1)}hH1_{(2-4)}$. (*D*) Steady-state cocaine block of the four channels. The pulse protocol is shown in the inset. The filled symbols are the averaged data for $\mu1_{(1-3)}hH1_{(4)}$ and $\mu1_{(1)}hH1_{(2-4)}$ measured in control saline. A Boltzmann function was used to fit the data obtained in the presence of 30 μm cocaine. The dotted lines are the fits to the averaged μ1 or hH1 data, and the open symbols and solid lines are the averaged data and fits to the channel chimera data. The average $V_{0.5}$ and k values for the fitted functions were: −92.1 ± 0.8 mV and 5.0 ± 0.2 mV, respectively for μ1; −115.4 ± 1.2 mV and 6.1 ± 0.2 mV, respectively, for hH1; −96.7 ± 0.7 mV and 5.5 ± 0.2 mV, respectively, for $\mu1_{(1-3)}hH1_{(4)}$; and −106.1 ± 0.9 mV and 7.6 ± 0.2 mV, respectively, for $\mu1_{(1)}hH1_{(2-4)}$.

TABLE 1 $V_{0.5}$ values of steady-state activation, inactivation, and cocaine block

Channel	Activation $V_{0.5}$ (mV)	Inactivation $V_{0.5}$ (mV)	Cocaine $V_{0.5}$ (mV)
μ1	$-32.8 \pm 2.8^{\#}$ (7)	$-78.5 \pm 1.0^{\#}$ (8)	$-92.1 \pm 0.8^{\#}$ (7)
hH1	-48.0 ± 1.8* (6)	-94.1 ± 1.4* (9)	-115.4 ± 1.2* (6)
$\mu1_{(1)}hH1_{(2-4)}$	$-32.4 \pm 0.6^{\#}$ (13)	-90.7 ± 1.0* (14)	$-106.1 \pm 0.9^{*\#}$ (15)
$\mu1_{(1-3)}hH1_{(4)}$	$-27.8 \pm 1.2^{\#}$ (11)	$-82.2 \pm 1.0^{*\#}$ (14)	$-96.7 \pm 0.7^{*\#}$ (8)
μ1-β1	$-31.1 \pm 0.8^{\#}$ (6)	$-69.0 \pm 0.6^{*\#}$ (8)	$-79.8 \pm 0.7^{*\#}$ (8)
hH1-β1	$-43.3 \pm 1.0^{*\S}$ (6)	$-81.2 \pm 1.7^{\#}$ (6)	$-100.4 \pm 1.4^{*\#}$ (6)

The $V_{0.5}$ values obtained for the channel chimeras and for the α subunits coexpressed with the β1 subunit were compared to those of the wild-type α subunits, μ1 and hH1.

$^{*\#}P < 0.05$ (Student's *t*-test) compared to μl or hH1, respectively.

$^{\S}P = 0.05$ compared to hH1. Numbers in parentheses indicate the number of cells.

resting $\mu1_{(1-3)}hH1_{(4)}$ channels and 57.6 ± 1.0% ($n = 6$) of resting $\mu1_{(1)}hH1_{(2-4)}$ channels. After a 10-s conditioning pulse to −70 mV, 300 μM cocaine blocked 96.4 ± 1.0% ($n = 5$) and 98.2 ± 2.8% ($n = 6$) of inactivated $\mu1_{(1-3)}hH1_{(4)}$ and $\mu1_{(1)}hH1_{(2-4)}$ channels, respectively. There was no significant difference ($p > 0.05$) in block between the two chimeras; nor was there a difference between the block of the chimeras and block of the wild-type channels. At intermediate voltages, where there was a mixture of resting and inactivated channels, the relative differences in 30 μM cocaine block among the four channels (Fig. 1 *D*) generally resembled the differences among the channels in steady-state inactivation (Fig. 1 *C*). Note that cocaine block of the $\mu1_{(1-3)}hH1_{(4)}$ chimera, which has domain 4 from hH1 and thus the putative local anesthetic receptor for hH1 (Ragsdale et al., 1994), more closely resembled cocaine block of μ1 channels. The differences in steady-state inactivation therefore provided a reasonable correlation for the observed differences in steady-state cocaine block.

Effects of β1 subunit coexpression on channel kinetics and cocaine block

In other expression systems, coexpression of the rat brain β1 subunit with the α subunit of sodium channels most often shifted channel kinetics toward more negative voltages. In *Xenopus* oocytes, coexpression of the β1 subunit with the α subunits of rat brain IIA (Isom et al., 1992) or μ1 (Nuss et al., 1995a) sodium channels increased current amplitude, speeded the rate of current decay, and shifted the voltage dependence of steady-state inactivation to more negative voltages. In Chinese hamster cells, β1 subunit coexpression with the rat brain IIa α subunit caused negative shifts in both activation and inactivation, but did not obviously affect the rate of current decay (Isom et al., 1995). Furthermore, in the oocyte expression system β1 subunit coexpression with hH1 channels reduced the resting affinity for lidocaine by twofold (Makielski et al., 1996).

Our first objective was to determine what effect, if any, β1 subunit coexpression had on the channel kinetics of μ1 or hH1 when expressed in HEK cells. Although β1 coexpression with μ1 and hH1 in HEK cells increased current amplitude as in other expression systems, there were surprisingly different effects on channel activation and inactivation. The $V_{0.5}$ values of activation for μ1-β1 and hH1-β1 were 2 mV and 5 mV, respectively, more positive than the $V_{0.5}$ values of activation for the α subunits alone (Fig. 2 *A*). Compared to the $V_{0.5}$ values of activation for μ1 and hH1 α subunits, the positive shift was modest (μ1 versus μ1-β1, $p > 0.05$; hH1 versus hH1-β1, $p = 0.05$). β1 subunit coexpression had virtually no effect on the time constant of macroscopic current decay during depolarizations to between 0 and +50 mV (Fig. 2 *B*). Coexpression of the β1 subunit with μ1 and hH1 channels induced strong positive shifts in the $V_{0.5}$ values of steady-state inactivation, as compared to expression of the α subunits alone (Fig. 2 *C*). For μ1-β1 and hH1-β1, the $V_{0.5}$ values of inactivation were, respectively, 10 mV ($p < 0.05$) and 13 mV ($p < 0.05$) more positive than the $V_{0.5}$ values of μ1 and hH1 (Table 1).

Because β subunit coexpression with μ1 and hH1 elicited strong positive shifts in steady-state inactivation and modest shifts in channel activation, we examined whether the β1 subunit altered the relationship between the conditioning voltage and cocaine block. Consistent with the effect on steady-state inactivation, β1 subunit coexpression with μ1 and hH1 induced strong positive shifts in the $V_{0.5}$ values of cocaine block. (Fig. 2 *D*). We changed the voltage range over which we examined cocaine block by 20 mV in the positive direction. Because the change in pulse protocol elicited more slow inactivation from μ1-β1 channels than from hH1-β1 channels, we normalized the block at each conditioning voltage by dividing the amplitude of the test current evoked in 30 μM cocaine by the amplitude of the test current evoked in control saline. The $V_{0.5}$ values of steady-state cocaine block at μ1-β1 and at hH1-β1 were 12 mV and 15 mV, respectively, more positive than the $V_{0.5}$ values of cocaine block at μ1 and hH1. Compared to block of the α subunits of μ1 and hH1, coexpression of the β1 subunit did not significantly ($p > 0.05$) alter the percentages of resting or inactivated channels blocked by either 30 μM (Fig. 2 *D*) or 300 μM cocaine. At −160 mV, 300 μM cocaine blocked 54.5 ± 1.5% ($n = 4$) of resting μ1-β1 channels and 54.9 ± 2.3% ($n = 4$) of resting hH1-β1 channels. After a 10-s conditioning pulse to −60 mV, 300 μM cocaine blocked 98.0 ± 1.0% ($n = 4$) and 97.1 ± 0.3%

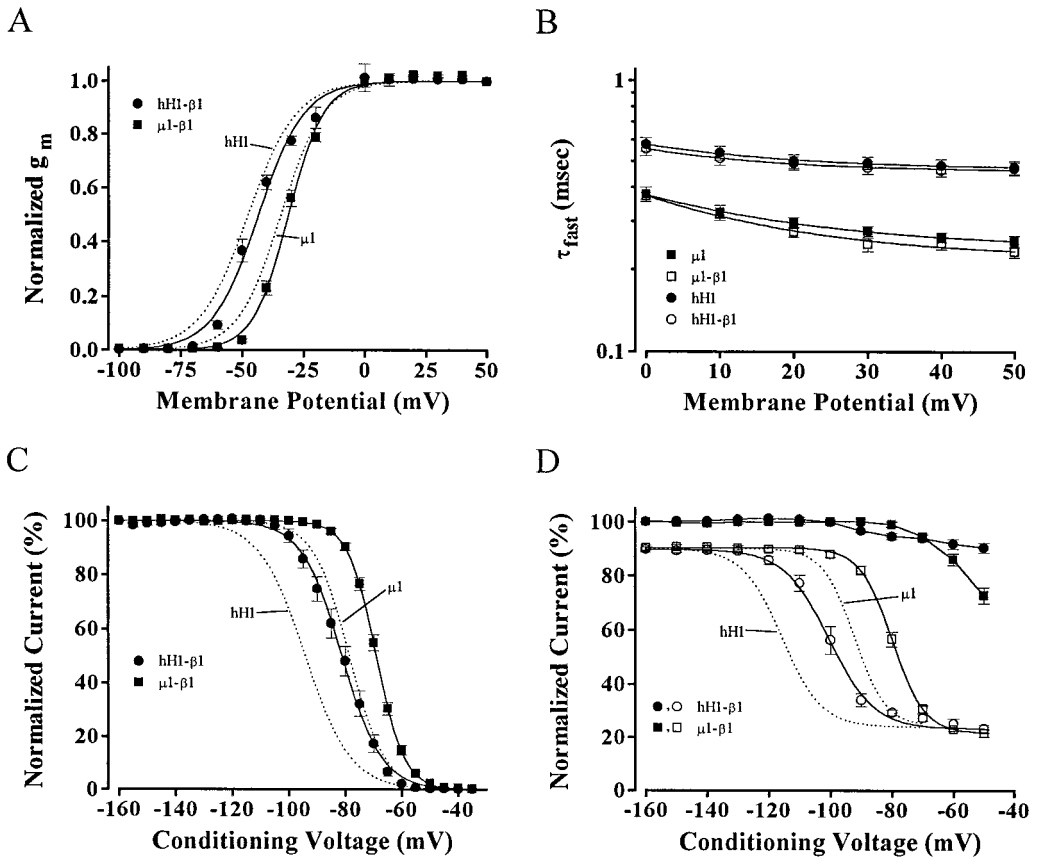

FIGURE 2 Effects of rat brain β1 subunit coexpression on μ1 and hH1 channel kinetics and cocaine block. (*A*) Normalized conductance of the α subunits of μ1 and hH1 channels with and without coexpression of the β1 subunit. The average $V_{0.5}$ and k values of the fitted Boltzmann functions to the μ1-β1 data were -31.1 ± 0.8 mV and 7.1 ± 0.2 mV, respectively, and these values for hH1-β1 were -43.3 ± 1.0 mV and 9.2 ± 0.7 mV, respectively. (*B*) Time constants of macroscopic current decay plotted versus the amplitude of 10-ms depolarizations. (*C*) Normalized sodium current availability (h_∞) function plotted versus the amplitude of the 100-ms conditioning pulse. Coexpression of the β1 subunit with μ1 or hH1 channels produced rightward shifts in the voltage dependence of channel inactivation. The average $V_{0.5}$ and k values of the Boltzmann function fitted to the μ1-β1 data were -69.0 ± 0.7 mV and 4.9 ± 0.2 mV, respectively, and these values for hH1-β1 were -81.2 ± 1.7 mV and 6.8 ± 0.2 mV, respectively. (*D*) Steady-state cocaine block. The filled symbols are the averaged data for μ1-β1 and hH1-β1 measured in control saline. The open symbols and solid lines are the averaged data and Boltzmann fits to the μ1-β1 and hH1-β1 data, and the dotted lines are the fits to the averaged data from μ1 and hH1 α subunits expressed alone (as in Fig. 1 *D*). The average $V_{0.5}$ and k values of the μ1-β1 data were -79.8 ± 0.7 mV and 5.1 ± 0.4 mV, respectively, and these values for hH1-β1 were -100.4 ± 1.4 mV and 6.2 ± 0.3 mV, respectively.

($n = 4$) of inactivated μ1-β1 and hH1-β1 channels, respectively. Thus, coexpression of the β1 subunit with μ1 or hH1 did not alter the cocaine affinities of either resting or inactivated channels. For the six sodium channels listed in Table 1, we plotted the $V_{0.5}$ values of cocaine block as a function of their respective $V_{0.5}$ values of activation and inactivation (Fig. 3). Regression analyses showed that the voltage dependence of steady-state cocaine block was better correlated with the voltage dependence of steady-state inactivation ($R = 0.98$) than with channel activation ($R = 0.66$).

Comparison of block recovery and use-dependent block at μ1 and hH1 channels

While the steady-state interactions between cocaine and cardiac sodium channels appear to be important in cocaine-induced cardiotoxicity, other interactions between cocaine and cardiac sodium channels may augment the cardiotoxic effects of cocaine. The fact that cardiac excitability is rhythmic and that cardiac cells spend more time than other sodium channel isoforms in the inactivated state suggests that the recovery time course from inactivated channel block and/or use-dependent block of cardiac sodium channels by local anesthetics may influence the net effects of cocaine. We therefore examined the recovery time course from cocaine block or in the extent of use-dependent block.

To determine the unbinding rate of cocaine from inactivated μ1 and hH1 channels, we delivered a 10-s conditioning pulse to -70 mV and measured the time-dependent recovery of current at -140 mV (Fig. 4, *inset*). The data obtained in control saline (*filled symbols*) showed that, in addition to eliciting fast inactivation, the conditioning pulse produced a slight amount of slow inactivation of both μ1 and hH1 channels. For both μ1 and hH1, the recovery from inactivation was best fitted by the sum of two exponentials. In control saline, the fast time constant of recovery was

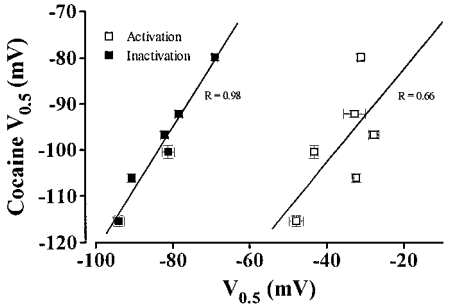

FIGURE 3 Dependence of cocaine block on channel kinetics. The $V_{0.5}$ values of 30 μM cocaine block of μ1, hH1, $\mu1_{(1)}$hH1$_{(2-4)}$, $\mu1_{(1-3)}$hH1$_{(4)}$, μ1-β1, and hH1-β1 channels were plotted versus the $V_{0.5}$ values of steady-state inactivation and activation of the channels. The error bars for the *x*-axis correspond to the standard errors of the averaged $V_{0.5}$ values of inactivation or activation. Linear regression analyses of the plots showed that the $V_{0.5}$ values of cocaine block were better correlated with the $V_{0.5}$ values of steady-state inactivation ($R = 0.98$) than with the $V_{0.5}$ values of steady state activation ($R = 0.66$).

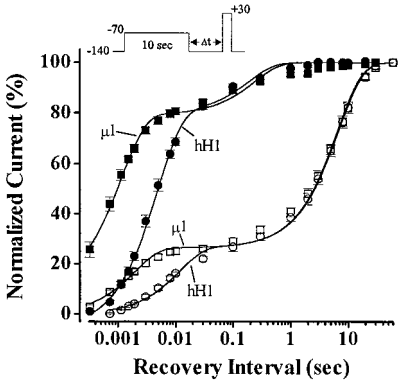

FIGURE 4 Recovery from cocaine block of inactivated channels. From a holding potential of −140 mV, μ1 (*squares*) and hH1 (*circles*) channels were stepped to −70 mV for 10 s. After a variable recovery interval at −140 mV, the channels were stepped to +30 mV to measure the available current. The recovery time courses in control saline (*filled symbols*) and in 30 μM cocaine (*open symbols*) were best fitted by the sum of two exponentials. In control saline, μ1 channels recovered with fast and slow time constants of 1.0 ± 0.1 ms and 279.1 ± 40.5 ms, respectively, and the fractional amplitude of the fast time constant comprised 81.2 ± 1.3% of the recovery; hH1 channels had fast and slow time constants of 6.3 ± 0.4 ms and 724.9 ± 190.0 ms, respectively, and the fractional amplitude of the fast time constant was 87.9 ± 1.9% of the recovery. In 30 μM cocaine, μ1 channels recovered with fast and slow time constants of 2.0 ± 0.2 ms and 6.5 ± 0.4 s, respectively, and the fractional amplitude of the fast time constant was 26.3 ± 1.4% of the recovery; hH1 channels recovered with fast and slow time constants of 11.5 ± 1.5 ms and 6.8 ± 0.5 s, respectively, and the fractional amplitude of the fast time constant was 27.5 ± 1.4% of the recovery.

1.0 ± 0.1 ms ($n = 5$) for μ1 channels and was 6.3 ± 0.4 ms ($n = 6$) for hH1 channels. These recovery rates were similar to the recovery rates for μ1 (1.5 ± 0.1 ms; $n = 5$) and hH1 (4.3 ± 0.7 ms; $n = 6$) after delivery of a 10-ms conditioning pulse to +30 mV. In control saline (see Fig. 6, *filled symbols*), the fast phase of recovery from inactivation for μ1 and hH1 channels comprised 81.2 ± 1.3% and 87.9 ± 1.9%, respectively, of the fractional amplitudes of recovery. The slow time constants of recovery for μ1 and hH1 channels were 279.1 ± 40.5 ms and 724.9 ± 190.0 ms ($p = 0.07$), respectively.

The recovery from 30 μM cocaine block also was best described as the sum of two exponentials. The fractional amplitudes of the fast time constants of recovery from cocaine block of μ1 and hH1 channels were 26.3 ± 1.4% and 27.5 ± 1.4% ($p > 0.05$), respectively. As with recovery from lidocaine block (Wright et al., 1997), we assumed that the fast time constants of recovery in the presence of 30 μM cocaine represented the recovery of drug-free channels and that the fractional amplitude of block at the conclusion of the fast phase of recovery represented block of inactivated channels. The fast time constants of recovery for μ1 and hH1 were 2.0 ± 0.2 ms and 11.5 ± 1.5 ms, respectively. This slowing of the fast time constant of recovery in the presence of cocaine also occurs in the presence of lidocaine and its quaternary derivatives (Yeh and Tanguy, 1985) and suggests that local anesthetics might affect the recovery from inactivation at "drug-free" channels by binding to them at various time points of the recovery phase. The time constant of recovery from cocaine block was similar for the two channels and required several seconds. The time constants of recovery from 30 μM cocaine block of μ1 and hH1 channels were 6.5 ± 0.4 s ($n = 5$) and 6.8 ± 0.5 s ($n = 6$; $p > 0.5$), respectively. These values were consistent with the time constant of cocaine unbinding from ventricular myocyte sodium channels (Crumb and Clarkson, 1990).

We compared use-dependent cocaine block of μ1 and hH1 channels using 1 and 2 Hz stimulation rates (Fig. 5) but found no difference between the channels in the extent of use-dependent block. Cells were held at −140 mV and received 25 ms pulses to +30 mV. Little use-dependent decrease in μ1 or hH1 sodium current occurred during 1- or 2-Hz stimulation in control saline, whereas repetitive pulses delivered in 30 μM cocaine produced potent use-dependent block. Use-dependent block of μ1 and hH1 channels by 30 μM cocaine was fitted by a single exponential function. The percentages of steady-state block at 1- and 2-Hz stimulation were 39.4 ± 1.8% and 50.1 ± 1.6%, respectively, for μ1 channels and were 41.5 ± 1.7% and 53.2 ± 1.3%, respectively, for hH1 channels. The difference in the percentage of steady-state block between μ1 and hH1 at either 1- or 2-Hz stimulation was not statistically significant ($p > 0.05$). Although increasing the duration of the depolarization would have increased the percentage of block at steady state, the relative similarities in use-dependent block of μ1 and hH1 channels would not likely have changed. When we delivered a single conditioning pulse to +30 mV for 300 ms followed by a 100-ms interval at the holding potential and a test pulse to +30 mV, cocaine blocked a similar percentage of μ1 channels (29.7 ± 2.0%; $n = 7$) and hH1 channels (24.6 ± 1.0%; $n = 5$; $p > 0.05$). Although there were no significant differences between μ1 and hH1 in the time course of recovery from block or in use-dependent block,

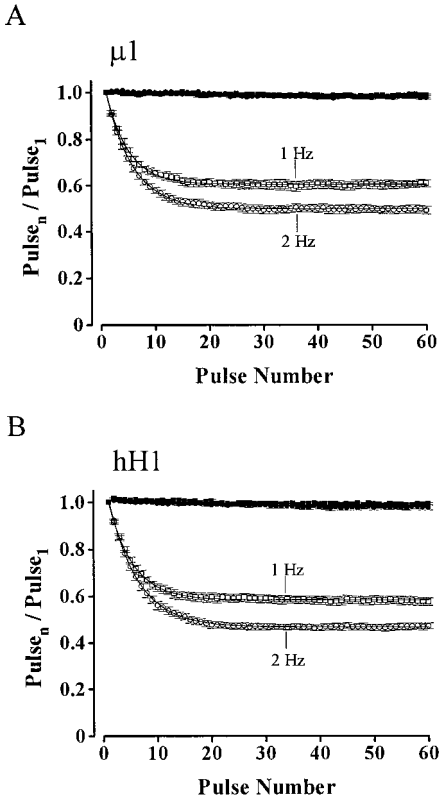

FIGURE 5 Use-dependent cocaine block of μ1 and hH1 channels. Sixty pulses to +30 mV were delivered to μ1 channels (*A*) and to hH1 channels (*B*) at stimulation frequencies of 1 and 2 Hz. In control saline (*filled symbols* in *A* and *B*), the pulse protocol did not elicit use-dependent decreases in current amplitude at either 1 or 2 Hz. The development of use-dependent block in 30 μM cocaine was best fitted by a single exponential function. (*A*) Use-dependent cocaine block of μ1 channels developed with a time constant of 4.1 ± 0.3 pulses and reached steady state at 39.4 ± 1.8% block during 1 Hz stimulation, and had a time constant of 4.9 ± 0.2 pulses and reached steady state at 50.1 ± 1.6% block during 2 Hz stimulation. (*B*) Use-dependent cocaine block of hH1 channels developed with a time constant of 4.5 ± 0.3 pulses and reached steady state at 41.5 ± 1.7% block during 1 Hz stimulation, and had a time constant of 5.4 ± 0.3 pulses and reached steady state at 53.2 ± 1.3% block during 2 Hz stimulation.

the extremely slow nature of the recovery from block (Fig. 4) and the extent of use-dependent block (Fig. 5) at hH1 channels suggest that these two parameters, in conjunction with the rhythmic cardiac action potential, may play significant roles in cocaine-induced cardiotoxicity.

Simulation of cocaine block using a modulated receptor model

In a previous report we attributed the differences in steady-state cocaine block between μ1 and hH1 to the differences in their steady-state inactivation curves (Wright et al., 1997). The data in the present study appear to support our claim because the $V_{0.5}$ values of steady-state cocaine block were better correlated with the $V_{0.5}$ values of steady-state inactivation than with the $V_{0.5}$ values of activation. Furthermore, the shifts in steady-state inactivation did not alter the affinities of resting and inactivated channels. To determine whether we could predict the voltage dependence of cocaine block, we used the steady-state inactivation data from each channel, as well as the K_R and K_I values to simulate steady-state cocaine block. For the simulation, we first determined the apparent K_d using the h_∞ curve of each channel. That is,

$$1/K_{app} = h/K_R + (1 - h)/K_I \quad (1)$$

where K_{app} is the apparent K_d, and K_R and K_I are the K_d values at resting and inactivated channels, respectively. The parameters h and $1 - h$ are the fractional distributions of resting and inactivated channels, respectively, at a given conditioning voltage (Bean et al., 1983). We used 250 μM as the K_R value and 9 μM as the K_I value. Note that in Eq. 1 the fraction of inactivated channels ($1 - h$) has a larger influence on the apparent K_d than does the fraction of available channels (h), and thus imposes a leftward shift on the simulation. For example, at the conditioning voltage where $h = 0.9$ and $1 - h = 0.1$, the apparent K_d is 68 μM; when both h and $1 - h = 0.5$, the apparent K_d is 17 μM. Fig. 6 *A* shows the K_{app} curves for μ1 and hH1 channels.

We then used the K_{app} values from Eq. 1 and the Langmuir isotherm (Hille, 1992) to predict the percentage of available channels at a given cocaine concentration:

$$I_{Na} = K_{app}/([LA] + K_{app}), \text{ or} \quad (2)$$

$$I_{Na} = 1/[1 + ([LA]/K_{app})] \quad (3)$$

where I_{Na} is the peak current measured during the test pulse and [LA] is the cocaine concentration.

We applied the simulation to μ1 and hH1 channels and used the 30 μM and 300 μM cocaine data from Wright et al. (1997) to see how well the model fit the data. The solid lines in Figs. 6 *B* and *C*) are the results of the simulation using Eqs. 1 and 3, and the symbols are the percentages of available channels in 30 μM cocaine (*filled symbols*) and in 300 μM cocaine (*open symbols*). The simulation predicted steady-state cocaine block of μ1 channels within a few millivolts at the midpoint of block (Fig. 6 *B*), whereas steady-state cocaine block of hH1 channels was several millivolts more negative than predicted by the simulation (Fig. 6 *C*). Scheme A in Diagram 1 depicts the simplified model (Bean et al., 1983) that uses Eqs. 1 and 3 to predict cocaine block. Thus, even though Eq. 1 imposed a significant leftward shift on the K_{app} value, the simulation failed to account for an equilibrium shift toward the inactivated and blocked state. One of the defining characteristics of a modulated receptor (Hille, 1977) is that local anesthetic shifts the equilibrium from the resting and drug-bound state (R^*) toward the inactivated and drug-bound state (I^*) as depicted in Scheme B. The difference between the amount of block predicted by the initial simulation (Scheme A) and the actual amount of block may be indicative of an equilibrium shift in the $R^* \leftrightarrow I^*$ portion of Scheme B (Courtney, 1975). Note that we could not directly measure this equilibrium

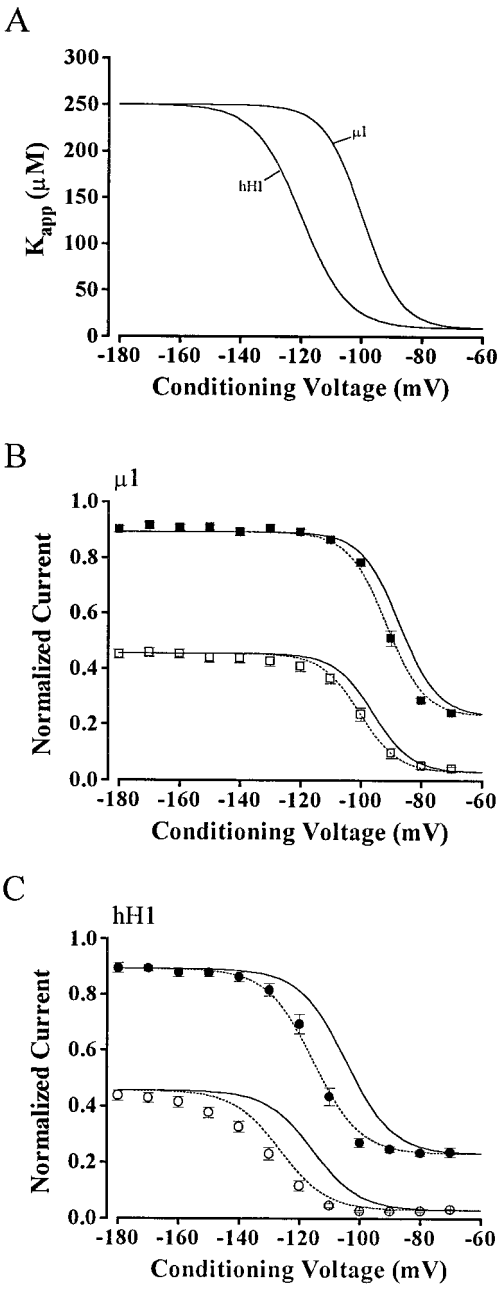

FIGURE 6 Simulations of cocaine block of μ1 and hH1 sodium channels. (*A*) Plot of the apparent K_d versus the conditioning voltage using Eq. 1. (*B*) and (*C*) The solid lines show the predictions of cocaine block of μ1 and hH1 channels using Eqs. 1 and 3. The filled symbols are the actual percentages of block by 30 μM cocaine, and the open symbols are the percentages of block by 300 μM cocaine. The dotted lines are the improved fits to the data after imposing shifts of −4.5 mV and −10 mV on the h_∞ curves of μ1 and hH1, respectively. See text for details.

shift because channels in the *R** and *I** states do not conduct. To account for the additional equilibrium shift at the drug-bound states and to improve the fit by the model, we adjusted the h_∞ curves of μ1 and hH1 channels by trial and error. Adjusting the h_∞ curves of μ1 and hH1 channels by −4.5 mV and −10 mV, respectively, improved how well the model predicted cocaine block (*dotted lines* in Fig. 6, *B* and *C*).

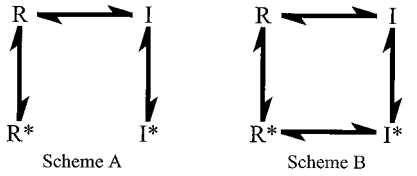

Diagram 1

We also used the model to simulate 30 μM cocaine block of the channel chimeras, μ1-β1 channels, and hH1-β1 channels (Fig. 7). The solid lines in Fig. 7, *A–D* show the predicted results using Eqs. 1 and 3 for 30 μM cocaine block of $\mu1_{(1-3)}hH1_{(4)}$, $\mu1_{(1)}hH1_{(2-4)}$, μ1-β1, and hH1-β1 channels. Introducing equilibrium shifts of −5 mV and −6 mV, respectively, to the h_∞ curves of $\mu1_{(1-3)}hH1_{(4)}$ and $\mu1_{(1)}hH1_{(2-4)}$ channels improved the prediction (Fig. 7, *A* and *B*, *dotted lines*). As with μ1 and hH1 channels, applying equilibrium shifts of −4.5 mV and −10 mV to the h_∞ curves of μ1-β1 and hH1-β1 channels, respectively, improved the prediction by the model (Fig. 7, *C* and *D*, *dotted lines*). Fig. 8 plots the average $V_{0.5}$ values of cocaine block versus the average $V_{0.5}$ values of steady-state inactivation. Each symbol corresponds to the averaged data from one of the isoforms in the study (see Fig. 8 legend). The cross symbol directly above each data point is the corresponding $V_{0.5}$ value of cocaine block as predicted by the simple model (Scheme A). The simulation results in Figs. 6–8 show that the equilibrium shift was larger for hH1 and hH1-β1 channels than for any of the other channels, suggesting that a larger equilibrium shift from *R** to *I** at the hH1 isoform may be an important factor in cocaine-induced cardiotoxicity (see Discussion).

DISCUSSION

In a previous paper (Wright et al., 1997), we showed that mammalian isoforms of cardiac and skeletal muscle sodium channel had similar resting and inactivated affinities for cocaine and lidocaine. This was in contrast to other studies (Nuss et al., 1995b; Wang et al., 1996b) which suggested that the sodium channels in cardiac tissue have a greater affinity for lidocaine compared to other sodium channel isoforms, and that this greater affinity might explain why cardiac tissue is relatively more sensitive than skeletal muscle to certain local anesthetics. We suggested that the differences in steady-state inactivation between hH1 channels and μ1 channels may in part explain the cardiotoxic effects of cocaine.

In the present study we further addressed state-dependent cocaine block of μ1 and hH1 sodium channels by focusing on the mechanisms responsible for the greater cocaine block of the hH1 isoform at intermediate voltages. First, we used shifts in the steady-state inactivation of μ1 and hH1 channels as a tool for investigating steady-state cocaine block. We induced shifts in steady-state inactivation by creating μ1/hH1 channel chimeras and also by coexpressing the rat

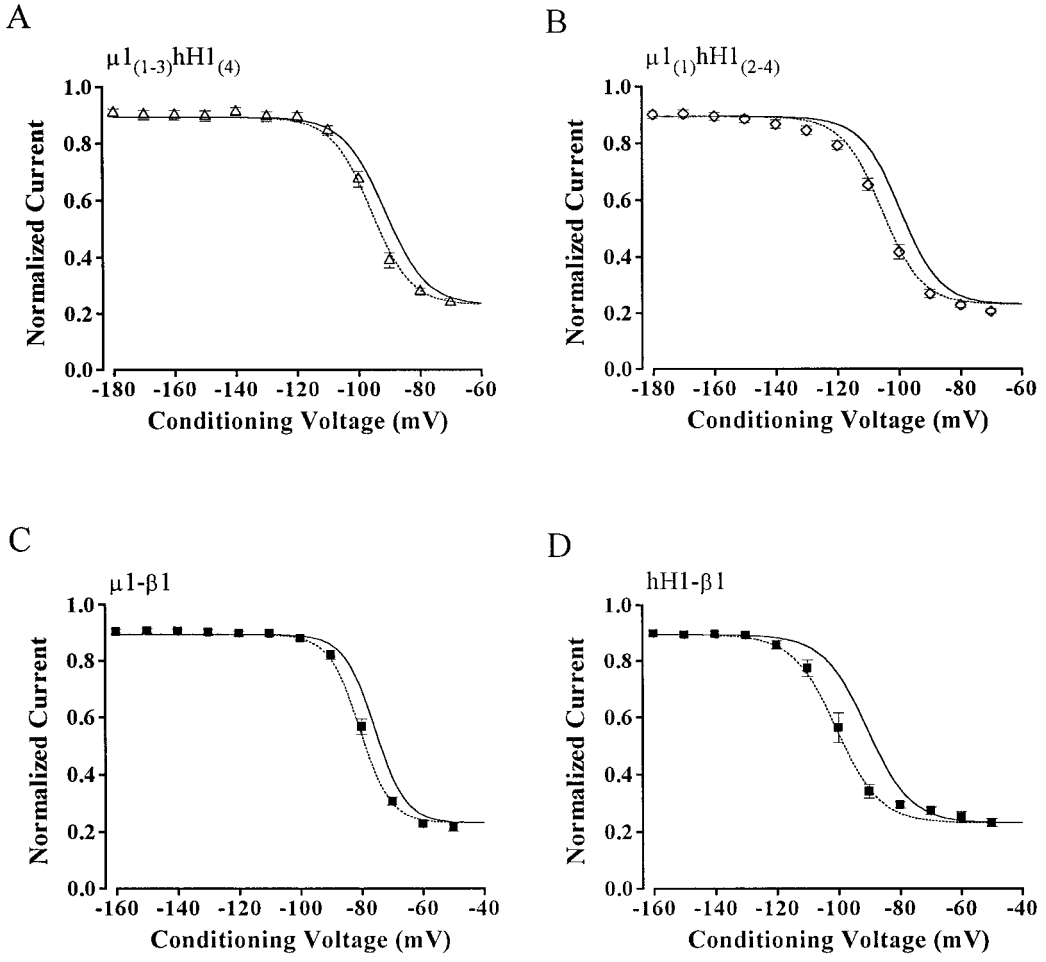

FIGURE 7 Simulations of cocaine block of channel chimeras and channels coexpressed with the β1 subunit. As described in Fig. 6, the apparent K_d at each channel was first determined using Eq. 1. (*A–D*) The solid lines show the predictions of cocaine block by 30 μM cocaine, and the dotted lines show the improved fits after imposing negative shifts in the h_∞ curves. The shifts for $\mu1_{(1-3)}$hH1$_{(4)}$, $\mu1_{(1)}$hH1$_{(2-4)}$, μ1-β1, and hH1-β1 channels were -5 mV, -6 mV, -4.5 mV, and -10 mV, respectively.

brain β1 subunit with the α subunits of μ1 or hH1. The shifts in the midpoint voltage of steady-state inactivation produced by these methods elicited directionally similar shifts in the midpoint voltage of cocaine block. Second, unlike several previous studies conducted with other expression systems, β1 subunit coexpression with the μ1 or hH1 α subunits in HEK cells shifted the voltage dependence of steady-state inactivation to more positive voltages, rather than toward more negative voltages, and did not affect the time constant of macroscopic current decay. In addition, coexpression of the β1 subunit did not alter the cocaine affinities of either resting or inactivated channels. And third, we used the h_∞ curves, the K_d values at resting and inactivated channels, and the Langmuir isotherm to simulate steady-state cocaine block.

Effects of channel chimera structure and β1 subunit coexpression on channel kinetics

We found it interesting that channel activation for both $\mu1_{(1-3)}$hH1$_{(4)}$ and $\mu1_{(1)}$hH1$_{(2-4)}$ resembled the activation kinetics of μ1 channels. Because $\mu1_{(1)}$hH1$_{(2-4)}$ contains only domain 1 from μ1 channels, it would be tempting to speculate that domain 1 is the crucial domain for determining channel activation. However, Chahine et al. (1996) and Benzinger et al. (1997) have also shown that the activation of several different μ1/hH1 channel chimeras each resembled the activation of μ1. Recently, Mitrovic et al. (1998) used cysteine point mutation within D2S4 and subsequent treatment with a cysteine modifying agent to demonstrate that domain 2 plays a significant role in channel activation. The findings by Mitrovic et al. (1998) and the data in Fig. 1 *B* argue against the hypothesis (Marcotte et al., 1997) that activation begins by outward movement of the S4 segment containing the most charged residues (domain 4) and concludes with the outward movement of the S4 segment with the fewest charged residues (domain 1). If this type of sequential movement of S4 segments occurred, then the activation phenotype of $\mu1_{(1)}$hH1$_{(2-4)}$ should have resembled the activation of hH1 channels rather than μ1 channels. These data suggest that channel activation is much more complex than can be deduced from the number of charged

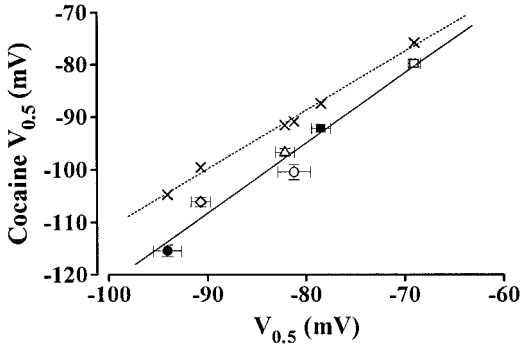

FIGURE 8 Plot of $V_{0.5}$ values of cocaine block versus the $V_{0.5}$ values of steady-state inactivation for the six channels in the study. As in Fig. 3, the solid line is the regression line through the plot of average $V_{0.5}$ values of cocaine block versus the average $V_{0.5}$ values of steady-state inactivation. In this figure, the individual channels are distinguished by a symbol (*filled square*, μ1; *open square*, μ1-β1; *filled circle*, hH1; *open circle*, hH1-β1; *open triangle*, $\mu 1_{(1-3)}hH1_{(4)}$; and *open diamond*, $\mu 1_{(1)}hH1_{(2-4)}$). The crosses are the predicted $V_{0.5}$ values of cocaine block using Eqs. 1 and 3 and the dotted line is the regression through the points. The cross symbol located directly above each data point corresponds to the predicted $V_{0.5}$ value of cocaine block for that particular channel. As discussed in the text, the predicted values for hH1 channels and hH1-β1 channels had the largest deviations from the measured data (*filled circle* and *open circle*, respectively).

residues in the S4 segments. One possible explanation for the discrepancy between our channel chimera data and the apparent importance of domain 2 in activation (Mitrovic et al., 1998) may be that domain regions from the μ1 isoform dominate the activation phenotype of channel chimeras constructed from μ1 and hH1.

The steady-state inactivation data obtained for μ1, hH1, and the channel chimeras indicate that the four domain regions have an evenly distributed role in determining the h_∞ phenotype (Fig. 1 *C*). The $V_{0.5}$ of steady-state inactivation for $\mu 1_{(1)}hH1_{(2-4)}$ channels was ~4 mV less negative than that of hH1, and the $V_{0.5}$ of inactivation for $\mu 1_{(1-3)}hH1_{(4)}$ channels was ~4 mV more negative than that of μ1. In another chimera study (Benzinger et al., 1997), the effects of a single domain substitution on steady-state inactivation phenotype seemed less clear because the $V_{0.5}$ values of steady-state inactivation for all chimeras were actually less negative than that of μ1. Although we were unable to test this phenomenon further using comparable channel chimeras ($hH1_{(1)}\mu 1_{(2-4)}$ and $hH1_{(1-3)}\mu 1_{(4)}$), the present data suggest that each domain contributes, perhaps equally, to the steady-state inactivation phenotype.

The shifts in the voltage dependence of activation and/or steady-state inactivation after coexpression of sodium channel α subunits with the rat brain β1 subunit appear to vary depending on the expression system and perhaps also on the sodium channel isoform. Coexpression of the β1 subunit shifted the activation and inactivation kinetics of rat brain sodium channels to more negative voltages in *Xenopus* oocytes (Isom et al., 1992) and in Chinese hamster cells (Isom et al., 1995). β1 subunit coexpression with μ1 channels in oocytes also elicited a negative shift in the voltage dependence of steady-state inactivation (Nuss et al., 1995a). In oocytes, the effect of β1 subunit coexpression with cardiac sodium channels varies from no shift in the steady-state inactivation of hH1 channels (Nuss et al., 1995b) or rat heart sodium channels (rH1; Qu et al., 1995) to one report of a modest but significant positive shift for hH1 channels (Makielski et al., 1996). In contrast to these studies, we found that coexpression of the β1 subunit with sodium channel α subunits in HEK cells markedly shifted steady-state inactivation (Fig. 2 *C*) of μ1 and hH1 channels in the positive direction by ~10 mV and ~13 mV, respectively. We cannot presently explain the variable effects of β1 subunit coexpression on sodium channel kinetics. One possibility may be that cellular processes such as protein phosphorylation (see Cukierman, 1996 for review), which can affect channel kinetics, differ among different expression systems. Alternatively, the time-dependent negative shift in steady-state inactivation (Wang et al., 1996a) may be reduced or eliminated by β1 subunit coexpression.

The positive voltage shifts in steady-state inactivation produced by β1 subunit coexpression with μ1 and hH1 resulted in directionally similar shifts in cocaine block (Fig. 2 *D*). The average $V_{0.5}$ values of cocaine block for μ1-β1 and hH1-β1 were 12.3 mV and 15.0 mV, respectively, more positive than the $V_{0.5}$ values of cocaine block for the α subunits of μ1 and hH1. Also important, β1 subunit coexpression did not affect the cocaine affinities of either resting or inactivated channels. In contrast, β1 subunit coexpression with hH1 channels in the oocyte expression system decreased the affinity of resting channels for lidocaine by ~2-fold (Makielski et al., 1996); a result most likely due to a small (3–7 mV) positive shift in steady-state inactivation.

Steady-state cocaine block, the modulated receptor model, and cocaine-induced cardiotoxicity

The data in Figs. 1–3 indicated that shifts in the voltage dependence of steady-state inactivation induced linear shifts in the voltage dependence of steady-state cocaine block. The simple model (Scheme A in Diagram 1; Bean et al., 1983), which used the h_∞ curve and the K_d values at resting and inactivated channels, gave a fairly accurate prediction of steady-state cocaine block at μ1 channels ($V_{0.5}$ within ~5 mV), but gave a somewhat less accurate prediction at hH1 channels ($V_{0.5}$ within ~10 mV). Even though the $V_{0.5}$ values of cocaine block were shifted by ~−10 mV compared to the $V_{0.5}$ values of steady-state inactivation, the simple model failed to account for the entire equilibrium shift because it did not include the transitions between the R^* and I^* states (Scheme B). Thus, the difference between μ1 and hH1 channels in the size of the underestimated equilibrium shift may reflect the difference in the amount of cocaine-induced leftward shift in h_∞, which in our case becomes evident in the $V_{0.5}$ value of steady-state cocaine

block. For example, the $V_{0.5}$ values of steady-state inactivation at μ1 and hH1-β1 channels were similar at −79 mV and −81 mV, respectively, but the $V_{0.5}$ value of cocaine block was ~8 mV more negative for hH1-β1 channels than for μ1 channels. Indeed, these data suggest that the 15 mV difference between the $V_{0.5}$ values of steady-state inactivation at μ1 and hH1 (Wright et al., 1997), as well as a larger cocaine-induced shift in the h_∞ curve of hH1 channels contribute to cocaine-induced cardiotoxicity.

Although steady-state inactivation appears to play the major role in determining steady-state cocaine block, channel activation could be one of the factors responsible for the magnitude of the underestimation in h_∞ shift. Compare the $V_{0.5}$ value of steady-state inactivation to the $V_{0.5}$ value of cocaine block for each channel (Table 1), and note the interesting quantitative difference between μ1 and hH1. For μ1 channels the difference between the $V_{0.5}$ value of cocaine block and the $V_{0.5}$ value of steady-state inactivation was ~14 mV and for hH1 channels the difference was ~19 mV. These differences were essentially the same at μ1-β1 and hH1-β1 channels. For both of the channel chimeras, the difference between the $V_{0.5}$ value of steady-state cocaine block and the $V_{0.5}$ value of steady-state inactivation was ~15 mV. When we adjusted the h_∞ curves to improve the fit by the simple model, the shift in the h_∞ curve that best improved the fit to the cocaine data from μ1 and μ1-β1 channels was −4.5 mV, whereas the adjustment for hH1 and hH1-β1 channels was −10 mV. For $\mu 1_{(1)}hH1_{(2-4)}$ and $\mu 1_{(1-3)}hH1_{(4)}$, the adjustments were 5 and 6 mV, respectively, which more closely resembled the adjustment required for μ1 channels. The fact that μ1 channels and the channel chimeras had the same activation phenotype and required similar adjustments in h_∞ to improve the fit by the simple model suggests that channel activation may affect the magnitude of the underestimated shift. As the conditioning voltage becomes less negative, hH1 channels enter preopen or preactivated states, which may influence the equilibrium shift from R^* to I^*. However, at the μ1 isoform and at the chimeras, channel activation begins at voltages ~15 mV more positive than at the hH1 isoform, so these channels would therefore not enter the preactivated states at the same voltages. This possible role for activation in the equilibrium shift of the h_∞ curve is consistent with previous suggestions that activation is important in local anesthetic action (Starmer et al., 1984; Yeh and Tanguy, 1985).

The notion that state-dependent differences between cardiac and skeletal muscle sodium channels influence local anesthetic action in cardiac tissue has been previously reported for single batrachotoxin-modified sodium channels (Zamponi et al., 1993; Zamponi and French, 1993). In native channels, the antiarrhythmic properties of lidocaine and the cardiotoxic properties of cocaine most likely result from steady-state interactions with inactivated sodium channels at the diastolic membrane potential, as well as from use-dependent interactions with activated and inactivated channels during the cardiac action potential. Here, we present an additional mechanism wherein cocaine induces a larger shift in the h_∞ curve at cardiac sodium channels than at skeletal muscle sodium channels. This additional shift in h_∞ may arise from the coupling between channel activation and inactivation (O'Leary et al., 1995), both of which proceed at significantly more negative potentials in the cardiac isoform.

We thank Dr. Roland Kallen for the hH1 clone, Dr. James Trimmer for the μ1 clone, Drs. Lori Isom and William Catterall for the rat brain β1 subunit clone, and Dr. Stephen Cannon for providing the HEK293t cell line and the CD8-pih3m plasmid.

This work was supported by National Institutes of Health National Research Service Award GM18760 (to S.N.W.) and National Institutes of Health Grants GM35401 and GM48090 (to G.K.W.).

REFERENCES

Bean, B. P., C. J. Cohen, and R. W. Tsien. 1983. Lidocaine block of cardiac sodium channels. *J. Gen. Physiol.* 81:613–642.

Benzinger, G. R., C. L. Drum, L.-Q. Chen, R. G. Kallen, and D. A. Hanck. 1997. Differences in the binding sites of two site-3 sodium channel toxins. *Pflügers Arch.* 434:742–749.

Cannon, S. C., and S. M. Strittmatter. 1993. Functional expression of sodium channel mutations identified in families with periodic paralysis. *Neuron*. 10:317–326.

Catterall, W. A. 1995. Structure and function of voltage-gated ion channels. *Annu. Rev. Biochem.* 64:493–531.

Chahine, M., I., Deschene, L. Q. Chen, and R. G. Kallen. 1996. Electrophysiological characteristics of cloned skeletal and cardiac muscle sodium channels. *Am. J. Physiol.* 271:H498–H506.

Courtney, K. R. 1975. Mechanism of frequency-dependent inhibition of sodium currents in frog myelinated nerve by the lidocaine derivative GEA 968. *J. Pharmacol. Exp. Ther.* 195:225–236.

Crumb, W. J., Jr., and C. W. Clarkson. 1990. Characterization of cocaine-induced block of cardiac sodium channels. *Biophys. J.* 57:589–599.

Cukierman, S. 1996. Regulation of voltage-dependent sodium channels. *J. Membr. Biol.* 151:203–214.

Fozzard, H. A., and D. A. Hanck. 1996. Structure and function of voltage-dependent sodium channels: comparison of brain II and cardiac isoforms. *Physiol. Rev.* 76:887–926.

Frelin, C., P. Cognard, P. Vigne, and M. Lazdunski. 1986. Tetrodotoxin-sensitive and tetrodotoxin-resistant Na^+ channels differ in their sensitivity to Cd^{2+} and Zn^{2+}. *Eur. J. Pharmacol.* 122:245–250.

Gellens, M. E., A. L. George, Jr., L. Chen, M. Chahine, R. Horn, R. L. Barchi, and R. G. Kallen. 1992. Primary structure and functional expression of the human cardiac tetrodotoxin-insensitive voltage-dependent sodium channel. *Proc. Natl. Acad. Sci. USA.* 89:554–558.

Hamill, O. P., A. Marty, E. Neher, B. Sakmann, and F. J. Sigworth. 1981. Improved patch-clamp techniques for high-resolution current recording from cells and cell-free membrane patches. *Pflügers Arch.* 391:85–100.

Hille, B. 1977. Local anesthetics: hydrophilic and hydrophobic pathways for the drug-receptor reaction. *J. Gen. Physiol.* 69:497–515.

Hille, B. 1992. Ionic Channels of Excitable Membranes, 2nd ed. Sinauer Associates, Inc., Sunderland, MA.

Hodgkin, A. L., and A. F. Huxley. 1952. A quantitative description of membrane current and its application to conduction and excitation in nerve. *J. Physiol. (Lond.).* 117:500–544.

Isom, L. L., K. S. De Jongh, D. E. Patton, B. F. X. Reber, J. Offord, H. Charbonneau, K. Walsh, A. L. Goldin, and W. A. Catterall. 1992. Primary structure and functional expression of the β1 subunit of the rat brain sodium channel. *Science*. 256:839–842.

Isom, L. L., T. Scheuer, A. B. Brownstein, D. S. Ragsdale, B. J. Murphy, and W. A. Catterall. 1995. Functional co-expression of the β1 and type IIA α subunits of sodium channels in a mammalian cell line. *J. Biol. Chem.* 270:3306–3312.

Makielski, J. C., J. T. Limheris, S. Y. Chang, Z. Fan, and J. W. Kyle. 1996. Coexpression of β1 with cardiac sodium channel α subunits in oocytes decreases lidocaine block. *Mol. Pharmacol.* 49:30–39.

Makita, N., P. B. Bennett, Jr., and A. L. George, Jr. 1996. Multiple domains contribute to the distinct inactivation properties of human heart and skeletal muscle Na^+ channels. *Circ. Res.* 78:244–252.

Marcotte, P., L.-Q. Chen, R. G. Kallen, and M. Chahine. 1997. Effects of *Tityus serrulatus* scorpion toxin γ on voltage-gated Na^+ channels. *Circ. Res.* 80:363–369.

Mitrovic, N., A. L. George, and R. Horn. 1998. Independent versus coupled inactivation in sodium channels: role of the domain 2 S4 segment. *J. Gen. Physiol.* 111:451–462.

Nuss, H. B., N. Chiamvimonvat, M. T. Perez-Garcia, G. F. Tomaselli, and E. Marbán. 1995a. Functional association of the β1 subunit with human cardiac (hH1) and rat skeletal muscle (μ1) sodium channel α subunits expressed in *Xenopus* oocytes. *J. Gen. Physiol.* 106:1171–1191.

Nuss, H. B., G. F. Tomaselli, and E. Marbán. 1995b. Cardiac sodium channels (hH1) are intrinsically more sensitive to block by lidocaine than are skeletal muscle (μ1) channels. *J. Gen. Physiol.* 106:1193–1209.

O'Leary, M. E., L.-Q. Chen, R. G. Kallen, and R. Horn. 1995. A molecular link between activation and inactivation of sodium channels. *J. Gen. Physiol.* 106:641–658.

Qu, Y. S., L. L. Isom, R. E. Westenbroek, J. C. Rogers, T. N. Tanada, K. A. McCormick, T. Scheuer, and W. A. Catterall. 1995. Modulation of cardiac Na^+ channel expression in *Xenopus* oocytes by β1 subunits. *J. Biol. Chem.* 270:25696–25701.

Ragsdale, D. S., J. C. McPhee, T. Scheuer, and W. A. Catterall. 1994. Molecular determinants of state-dependent block of Na^+ channels by local anesthetics. *Science*. 265:1724–1728.

Starmer, C. F., A. O. Grant, and H. C. Strauss. 1984. Mechanisms of use-dependent block of sodium channels in excitable membranes by local anesthetics. *Biophys. J.* 46:15–27.

Tomaselli, G. F., N. Chiamvimonvat, H. B. Nuss, J. R. Balser, M. T. Perez-Garcia, R. H. Xu, D. W. Orias, P. H. Backx, and E. Marbán. 1995. A mutation in the pore of the sodium channel alters gating. *Biophys. J.* 68:1814–1827.

Trimmer, J. S., S. S. Cooperman, S. A. Tomiko, J. Zhou, S. M. Crean, M. B. Boyle, R. G. Kallen, Z. Sheng, R. L. Barchi, F. J. Sigworth, R. H. Goodman, W. S. Agnew, and G. Mandel. 1989. Primary structure and functional expression of a mammalian skeletal muscle sodium channel. *Neuron*. 3:33–49.

Wang, D. W., A. L. George, Jr., and P. B. Bennett. 1996a. Comparison of heterologously expressed human cardiac and skeletal muscle sodium channels. *Biophys. J.* 70:238–245.

Wang, D. W., L. Nie, A. L. George, Jr., and P. B. Bennett. 1996b. Distinct local anesthetic affinities in Na^+ channel subtypes. *Biophys. J.* 70: 1700–1708.

Wang, S.-Y., and G. K. Wang. 1997. A mutation in segment I-S6 alters slow inactivation of sodium channels. *Biophys. J.* 72:1633–1640.

Wright, S. N., S.-Y. Wang, R. G. Kallen, and G. K. Wang. 1997. Differences in steady-state inactivation between sodium channel isoforms affect local anesthetic binding affinity. *Biophys. J.* 73:779–788.

Wright, S. N., S.-Y. Wang, Y.-F. Xiao, and G. K. Wang. 1998. Relationships between steady-state inactivation, cocaine binding, and cocaine affinity at voltage-gated sodium channels. *Biophys. J. (Abstr).* 312.

Yeh, J. Z., and J. Tanguy. 1985. Sodium channel activation gate modulates slow recovery from use-dependent block by local anesthetics in squid giant axons. *Biophys. J.* 47:685–694.

Zamponi, G. W., D. D. Doyle, and R. J. French. 1993. State-dependent block underlies tissue specificity of lidocaine action on batrachotoxin-activated cardiac sodium channels. *Biophys. J.* 65:91–100.

Zamponi, G. W., and R. J. French. 1993. Dissecting lidocaine action: diethylamide and phenol mimic separate modes of lidocaine block of sodium channels from heart and skeletal muscle. *Biophys. J.* 65: 2339–2347.